Chinese Journal of Aeronautics, (2017), 30(1): 274–281

Chinese Society of Aeronautics and Astronautics
& Beihang University

Chinese Journal of Aeronautics

cja@buaa.edu.cn
www.sciencedirect.com

Experimental investigation on a cavity-step-actuated supersonic oscillating jet

Luo Xiaochen, Sun Bo *, Wang Xiang'ang

Department of Aerospace Engineering, Nanjing University of Science and Technology, Nanjing 210094, China

Received 3 August 2015; revised 28 November 2015; accepted 24 December 2015
Available online 21 December 2016

KEYWORDS

Jet cavity interactions;
Jet flipping;
Oscillating jet;
Supersonic jet;
Wind tunnel testing

Abstract Wind tunnel testing is conducted at different back pressures in a vacuum-type wind tunnel for a novel supersonic fluidic oscillator which consists of a two-dimensional Laval nozzle, a rectangular cavity and a backward step, to obtain its characteristics and the conditions for jet oscillating. The experimental results show that periodic asymmetrical flipping of the supersonic jet appears over certain nozzle pressure ratio (NPR) range according to schlieren visualization and pressure fluctuations. The jet flipping appears only when the jet is over expanded. The normalized average amplitude of the lateral pressure difference acting on the roofs of the cavity and the step varies around 0.2 while the periodic flipping appears. The supersonic jet periodic flipping frequencies obtained from the experiments agree well with those from the modified Rossiter mode for cavity-step acoustic resonance, but further investigations are needed to discover the underlying mechanism for the jet flipping.

1. Introduction

Fluidic oscillators, which produce an oscillating jet (sweeping or pulsing jet) at high frequency, are attracting increased attention in recent years due to their application potentials as flow control actuators.[1] The attractive features of fluidic oscillators for flow control are their characteristics of unsteady blowing, wide range of operating frequency, and the distributed nature of momentum addition. Innovative applications of fluidic oscillators to flow control problems include separation control,[2] jet thrust vectoring, cavity tone suppression, and so on.[3,4]

One characteristic of all fluidic oscillators is that there must be some type of feedback mechanism to drive the oscillations. Based on the difference in the feedback mechanism, at least four types of fluidic oscillators have been invented so far, i.e., wall attachment,[5] jet interaction,[6] cavity acoustic resonance, and vortex oscillators.[3] Wall attachment and jet interaction oscillators have received more investigations in recent years, and details on these two oscillators were summarized in two latest review papers.[3,4]

The cavity resonating oscillator was developed as one type of temperature sensor around the 1970's.[7] One typical design is

* Corresponding author.
E-mail addresses: luonuaa@163.com (X. Luo), hypersun@njust.edu.cn (B. Sun), 2213302759@qq.com (X. Wang).

Peer review under responsibility of Editorial Committee of CJA.

http://dx.doi.org/10.1016/j.cja.2016.12.010

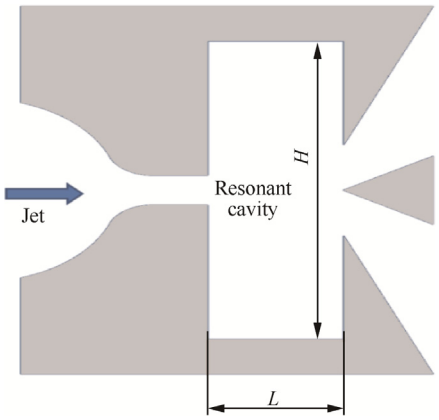

Fig. 1 Cavity resonating oscillator (redrawn based on Refs. 10,11).

shown in Fig. 1. As a fluid jet issues from the inlet nozzle and impinges on a wedge, it is subjected to an oscillation transversely to the jet issuing direction. This oscillation has traditionally been called edge tone oscillation.[8] The edge-tone oscillation is caused by inherent shear layer instabilities, vortex shedding, and acoustic feedback characteristics of the jet-edge configuration, and is dependent upon the jet velocity and the distance from the nozzle exit to the wedge.

The cavity in which the fluid runs from the inlet nozzle to the discharge exhaust has a characteristic or acoustic resonance frequency (eigen frequency). Carter[7] pointed out that this cavity eigen frequency is excited by the edge tone oscillations beginning at an input pressure corresponding to the threshold point. No distinct oscillation is produced until the input pressure reaches the threshold value. At this value, the frequencies of oscillations produced by the flow impinging on the edges at the exhaust begin to match the cavity eigen frequencies.

The acoustic resonance frequency for face-to-face cavities can be expressed by the cross junction mode[9] which depends on the acoustic velocity c and the cavity height H as follows:

$$f = mc/2H \tag{1}$$

where $m = 2n + 1$ ($n = 0, 1, 2, \ldots$). Since the sound speed is a function of temperature, the output frequency can be expressed by

$$f = \frac{m\sqrt{\gamma R_g T}}{2H} \tag{2}$$

where T is the temperature of the fluid in the cavity, γ is specific heat ratio and R_g is gas constant. Knowles[10] tested a cavity acoustic resonance oscillator which was similar to the one shown in Fig. 1 (L denotes the cavity length), and his results showed that the experimental frequency of oscillation agreed well with the prediction by Eq. (2).

As can be seen from Eq. (2), for a certain oscillator (i.e., H is fixed), the oscillation of the fluid in the cavity is a function solely of the temperature of the fluid which is usually constant for flow control applications, which means that the oscillating frequency for a given oscillator is fixed, without considering the influence of the integer m. This is beneficial for flow control applications,[1] compared to a wall attachment oscillator in which the oscillation frequency is directly dependent on the flow rate through the device.

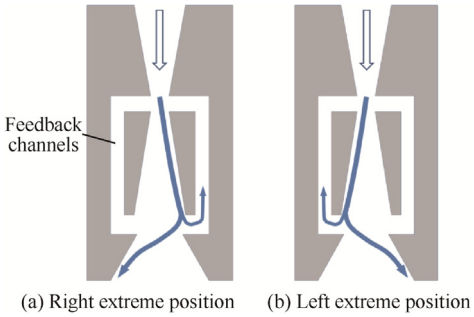

Fig. 2 Typical wall attachment oscillator (redrawn based on Ref. 13).

Several researches on cavity resonating oscillators in 1970's were limited in their subsonic operation. In recent work on wall attachment oscillators, only a few researchers investigated their operation of the supersonic flow. Raman et al.[12] reported their research on the extension of a " flip-flop" jet nozzle to supersonic flows. They made their device operate as a supersonic flapping jet at frequencies over 300 Hz. Oscillations stopped when the pressure ratio increased high sufficiently that the internal jet expanded enough to touch both side walls. Gokoglu et al.[13] reported their work related to the computational investigation of the internal flow in a fluidic oscillator (Fig. 2) working at supersonic conditions. Their two-dimensional (2D) simulations matched the oscillation frequencies measured from experiments across a wide range of pressure ratios. The existence of supersonic flow at the exit was verified, and the complex inner interactions between vortical structures and the feedback channels as well as the exit nozzle that led to oscillations were revealed by their computations.

Seele et al.[14] published schlieren photos in which a supersonic flow at the exit of a fluidic oscillator was clearly shown. We conducted supersonic jet flipping research on two novel symmetric supersonic fluidic oscillators which consisted of a 2D nozzle and two face-to-face cavities. The difference between these two is that one consisting of a 2D convergent nozzle and the other of a 2D Laval nozzle. Both oscillators were studied through wind tunnel tests to analyze the jet flipping. It was found that periodic supersonic jet flipping appeared under certain pressure condition and the oscillating jet achieved significant mixing enhancement.[15,16]

This paper focuses on the characteristics of supersonic operation of a cavity acoustic resonance oscillator with an innovative design to produce a sweeping jet. Different from our previous research, this supersonic fluidic oscillator is asymmetric. The operation limit and oscillating course of this innovative oscillator have been studied experimentally.

2. Oscillator geometry

Based on Carter's theory of coupling of edge-tone oscillation and Campagnuolo's[11] design (Fig. 1), an oscillator was designed and fabricated for the test. Different from the oscillator with a convergent nozzle from Carter's design, convergent-divergent nozzles were employed in this work and the wedge downstream from the exit was removed. The oscillator (Fig. 3) has a nozzle throat height of 5 mm and a nozzle divergence angle of 5°. At the exit of the nozzle, there are two face-

to-face backward steps. The lower step is partially covered by a 60° wedge, which forms a rectangular cavity with a length/depth ratio of 2.04. The oscillator has a width (z direction) of 40 mm.

3. Test facilities and instrumentations

A vacuum-type wind tunnel was used for all of the experiments. The inlet of the nozzle was exposed to the atmosphere with ambient pressure of 100.69–101.71 kPa and relative humidity of 18.0%–23.2%, whereas the outlet was connected to a vacuum tank (Figs. 3 and 4). The vacuum tank has a large volume of 33 m^3 and the back pressure of the nozzle is constant at the desired value during a typical test time of 1–2 s. In this paper, the nozzle pressure ratio (NPR) is defined as the ratio of ambient pressure at the nozzle entrance to the pressure in the vacuum tank.

A standard schlieren system was used to visualize the transient flow inside and downstream from the oscillator (Fig. 3). A light ray from a metal halide continuous light source (LS-M350, Sumita Optical Glass Inc.) passed the first plane mirror, two concave mirrors on each side of the nozzle, the second plane mirror, and a horizontal knife edge, reaching a high-speed video camera (Photron Fastcam MAXP01, 12500 frames per second, 1/120000 exposure speed). The Photron Fastcam Viewer interface was used for storing 1000 schlieren images of 0.08 s flow time.

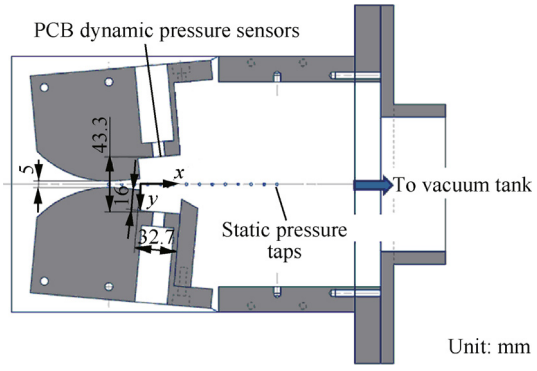

Fig. 3 Supersonic jet oscillator installed in a vacuum-type wind tunnel.

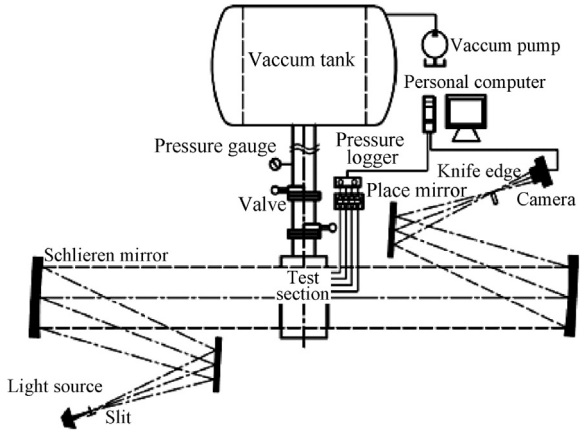

Fig. 4 Schematic of the wind tunnel system.

Two ICP dynamic pressure sensors (Model M101A05, PCB Piezotronics) were used to measure the unsteady pressures on the roofs of the cavity and the step. The sampling frequency was 50 kHz and the record time was 0.4 s. Fourteen pressure taps with a 10 mm interval on the centerline of a sidewall of the oscillator (Fig. 3) were connected to PG-2KU pressure transducers to measure the time average static pressure of the flow. The average static pressures were obtained based on 0.1 s measurement with a sampling frequency of 5000 Hz.

4. Results

The supersonic oscillator was tested from NPR = 2.5 to NPR = 7.8. Schlieren videos, unsteady pressures in the cavity and the step, and static pressures along the centerline of the oscillator were recorded for all the NPR cases. From the videos and the test data, the operation limit, oscillating course, and possible underlying mechanism of the supersonic oscillator were analyzed.

4.1. Flow visualization

Schlieren visualization recorded the qualitative flowfields of the oscillator at all NPRs. From the schlieren videos, continuous flipping between the cavity and the step of the supersonic jet was found to appear from NPR = 2.9 to NPR = 5.6. When NPR > 5.6, no obvious flipping was observed; while at NPR < 2.9, intermittent flipping of the supersonic jet tended to appear.

Fig. 5 gives schlieren sequences during almost one flipping period (T = 0.6039 ms) at NPR = 7.8. It should be noted that expansion waves occurred near the exit of the nozzle. It can be seen that at t/T = 0 (t is the time), the jet was nearly symmetrical in shape, and then the jet contracted. At t/T = 0.3974, the jet contracted to nearly minimum, and then began to expand. At t/T = 0.9273, the jet expanded to nearly the maximum in shape and finished one period. No apparent jet flipping could be seen.

Since only 4 photos were obtained in one period due to a lower sampling frequency, Fig. 6 gives schlieren sequences during almost two flipping periods (T = 0.2829 ms for one period) at NPR = 4.4. It can be seen that at t/T = 0, the jet nearly reached to its lower extreme position. The jet center impinged the rear wall of the cavity, so a part of the jet airflow was retarded and the pressure rose, which formed a lateral force and drove the jet flip upward. Then at t/T = 1.1311, the jet center was pushed to the upper step. At t/T = 0.5656, the jet center was deflected near the upper extreme position. At t/T = 1.6967, the jet centre was flipped downward. Finally, at t/T = 1.9794, the jet reached to its lower extreme position again. It could also be seen that there was an eddy near the rear edge of the step, different from the case at NPR > 5.6. The eddy, shedding periodically from the rear edge of the step, could play an important role in the jet flipping.

Fig. 7 gives schlieren sequences during 0.3586 ms at NPR = 2.54. It can be seen that the shock waves traveled along the axial direction of the nozzle over a larger range, with intermittent jet flipping. It should be noted that there was still an eddy near the rear edge of the step, different from the periodic flipping, but in this case, the eddy was more close to the roof of the step. It should also be noted that the jet flipping

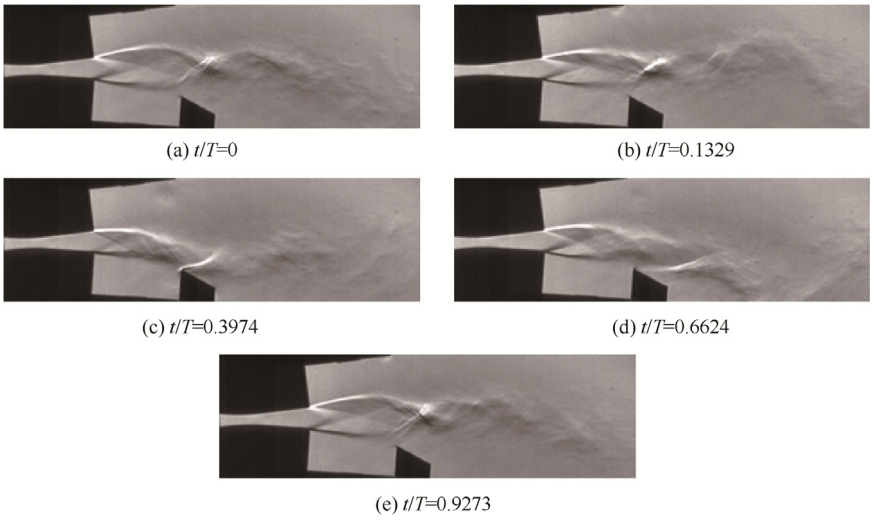

Fig. 5 Schlieren sequences of flow in the oscillator during one period or so at NPR = 7.8 (horizontal knife edge).

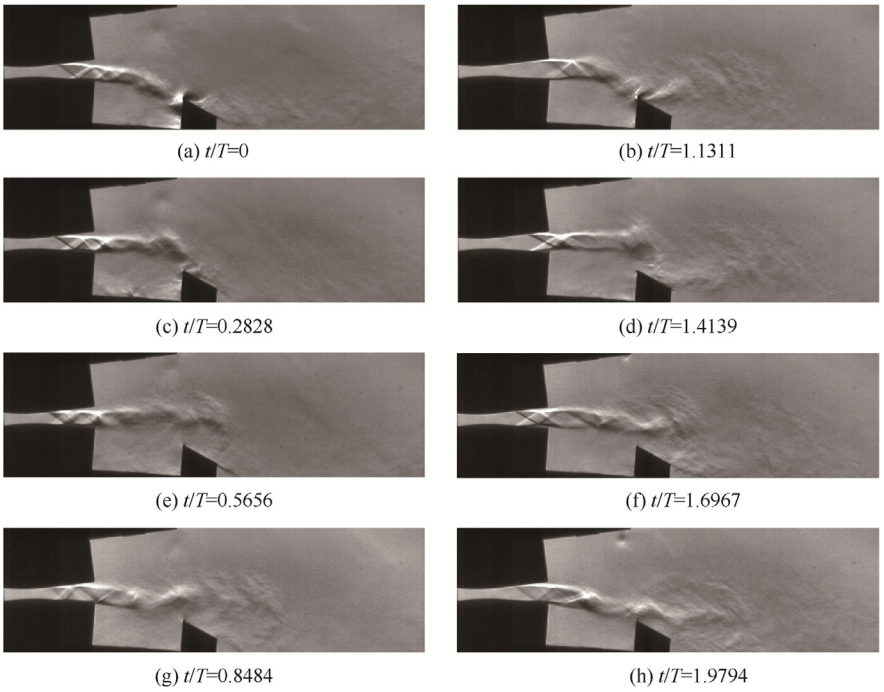

Fig. 6 Schlieren sequences of flow in the oscillator during two periods or so at NPR = 4.4 (horizontal knife edge).

was still apparently asymmetrical and the jet center was deflected to the cavity all the time.

4.2. Time average flow in the oscillator

Time average features of the unsteady flow in the oscillator were analyzed with static pressure measurements. Normalized static pressure p/p_a (normalized by the ambient pressure p_a at the nozzle entrance) distributions along the centerline of the oscillator at different NPR operations are shown in Fig. 8. In Fig. 8, x is the horizontal coordinate and h_t is the nozzle throat height. It can be seen that the pressure near the nozzle exit remained constant when NPR > 5.6 while increased gradually with NPR when NPR $\leqslant$ 5.6. That is, when NPR > 5.6, the jet was under-expanded; when NPR $\leqslant$ 5.6, the jet was over-expanded. For all the NPR cases, the pressures in the oscillator (denoted by the fourth to sixth pressure taps) was lower than the back pressure, due to the entrainment of the jet on the air in the oscillator.

Mach number at $x/h_t = 0$ just in the exit section of the nozzle was obtained based on the static pressure near that position, the assumption of isentropic flow in the jet, and linear interpolation. The jet Mach number at the exit section of the nozzle, varying with the NPR is given in Fig. 9. The jet Mach number for NPR = 5.6 is 1.96. Considering the jet Mach number with perfect expansion of 1.99, the above classification of

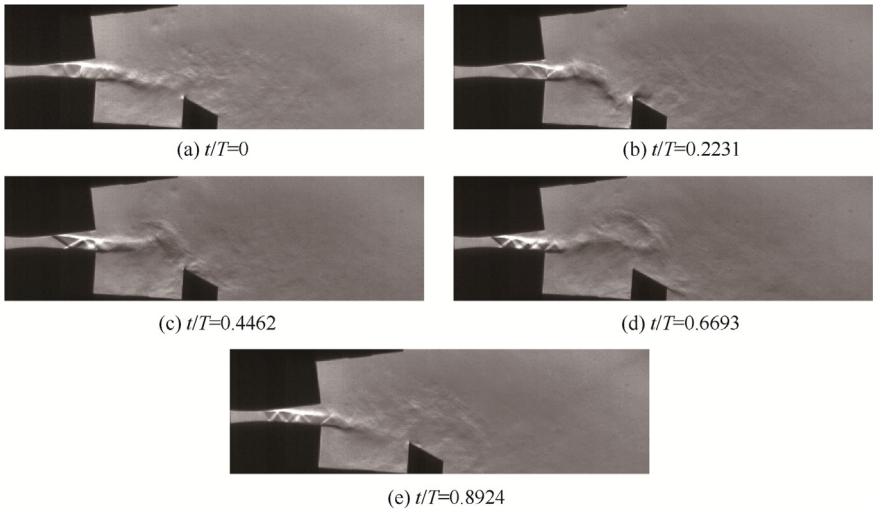

Fig. 7 Schlieren sequences of flow in the oscillator during 0.3586 ms at NPR = 2.5 (horizontal knife edge).

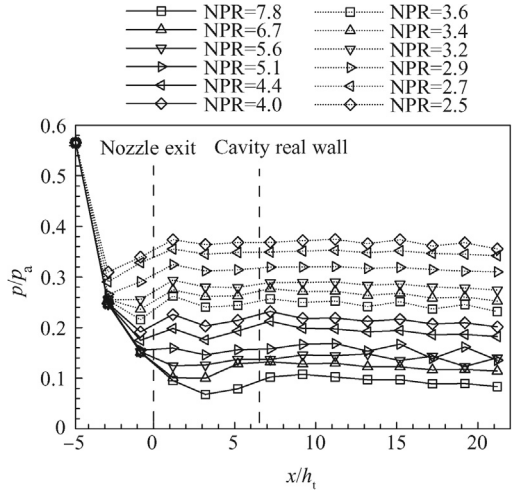

Fig. 8 Static pressure distributions along the centerline of the oscillator.

the jet was proven further. It might be argued that the jet flipping appeared only when the jet was over-expanded.

4.3. Possible underlying mechanism for an oscillator without a wedge

Similar to Carter's[7] theory for an oscillator with a wedge (Section 1), for an oscillator without a wedge (Fig. 10), the cross junction mode of cavity resonance could be excited by a cavity acoustic tone oscillation instead of an edge-tone oscillation.[17]

The cavity tone oscillation is caused by inherent shear layer instabilities, vortex shedding, and acoustic feedback characteristics of the cavity configuration.[18] The frequency of the cavity tone oscillation can be obtained by a semi-empirical equation which was developed by Rossiter[19] and has been modified by Heller and Bliss[20] for high-Mach number flows. The modified Rossiter formula takes the form of:

$$\frac{fL}{u}=\frac{n-\alpha}{\dfrac{Ma}{\sqrt{1+\left(\dfrac{r}{2}\right)(\gamma-1)Ma^2}}+\dfrac{1}{k_c}} \tag{3}$$

where f is the frequency at a given mode number n (n = 1, 2, 3,...); u is the jet velocity; r is the recovery factor; α and k_c are empirical parameters. The most commonly used values of α = 0.25, k_c = 0.57, and r = 0.89 were applied in this paper.

For cross junction flows with high Mach numbers, the cross junction mode denoted by Eq. (2) should be modified to take into account the difference between the air temperatures in the jet and the cavities. The jet temperature T_j can be given by

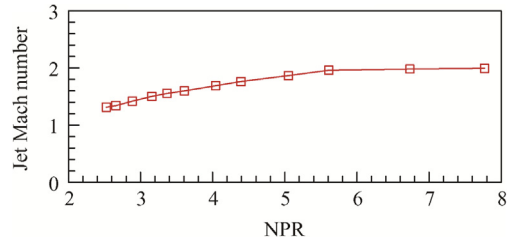

Fig. 9 Jet Mach number variations at different NPRs.

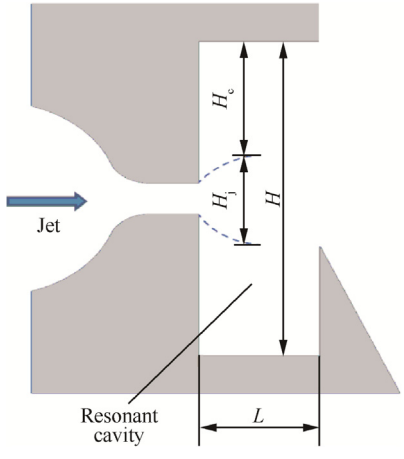

Fig. 10 Cavity resonating oscillator without a wedge.

$$T_j = \frac{T_a}{1 + \frac{\gamma - 1}{2} Ma_j^2} \tag{4}$$

where Ma_j is the jet Mach number; T_a is ambient temperature at the nozzle antrance.

The air temperature in the cavities T_c is the recovery temperature of the flow[20] which can be calculated by

$$T_c = T_a \left(r + \frac{1 - r}{1 + \frac{\gamma - 1}{2} Ma_j^2} \right) \tag{5}$$

Based on the two different temperatures, the frequencies of the cross junction mode for high Mach number flows can be written as

$$f = \frac{m}{\frac{2H_j}{c_j} + \frac{4H_c}{c_c}} \tag{6}$$

where H_j and H_c are the width of the jet and the depth of the cavity (Fig. 10), respectively. H_j is calculated based on the jet Mach number Ma_j and the conservation of mass flow rate. c_j and c_c are the sound speeds in the jet and the cavities, respectively, which are given by

$$c_j = \sqrt{\gamma R_g T_j} \tag{7}$$

$$c_c = \sqrt{\gamma R_g T_c} \tag{8}$$

4.4. Fluctuating pressure in the cavities

In general, the unsteady pressures acting on the roofs of the cavity and the step contain both random and periodic components. It has been reported that the periodic component is due to an acoustic resonance within the cavity excited by a phenomenon similar to that causing edge-tones.[19] The oscillating characteristics of the supersonic jet were analyzed based on fluctuating pressure measurements and the oscillating frequency estimation mentioned above. Pressure histories measured with PCB sensors on the roofs of the cavity and the step at NPR = 4.4 are shown in Fig. 11. The pressures were normalized by the jet kinetic pressure q in the exit section of the nozzle. The distributions of pressure fluctuations show that the wave forms of the upper step and lower cavity are similar; the unsteady pressures on the roofs of the cavity and the step are periodic in character and have a normalized average oscillating amplitude of about 0.15.

From the pressure fluctuations, continuous oscillating between the cavity and the step of the supersonic jet was found to appear from NPR = 2.5 to NPR = 5.6, among which, the jet oscillated periodically between the cavity and the step from NPR = 2.9 to NPR = 5.6. When NPR > 5.6, no obvious oscillating was observed; while at NPR < 2.9, intermittent oscillating of the supersonic jet tended to appear.

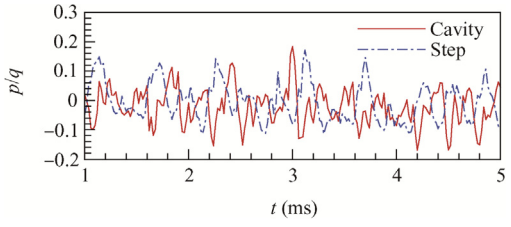

Fig. 11 Pressure fluctuations on the roofs of the cavity and the step at NPR = 4.4.

Before the amplitude of the jet oscillating can be estimated, it is necessary to know the magnitude of the lateral pressure difference p_1–p_2 acting on the jet. p_1 denotes the measured static pressure on the roof of the lower cavity; p_2 denotes the measured static pressure on the roof of the upper step.

The lateral pressure difference between the roofs of the cavity and the step at NPR = 7.8 is presented in Fig. 12(a). The pressure was also normalized by the jet kinetic pressure q. It can be seen that the unsteady p_1–p_2 contains both random and periodic components while the periodic component is in character. The periodic component is due to an acoustic resonance within the cavity excited by a phenomenon similar to that causing edge-tones.[19] The fluctuating pressure difference during the period seems to have the form of a sine wave. Fig. 12(b) presents the fluctuation of p_1–p_2 at NPR = 4.4. It might be argued that p_1–p_2 is the combination of periodic and random components in character and the periodic component predominates when the NPR varies from 2.9 to 5.6. The fluctuation of p_1–p_2 at NPR = 2.5 is indicated in Fig. 12(c) and it can be seen that the fluctuation of p_1–p_2 is non-periodic in character.

For a given cavity geometry, it might be argued that the magnitude of the unsteady lateral pressure difference was proportional to incoming flow kinetic pressure.[19] Fig. 13 presents the averaged amplitude of p_1–p_2 at an NPR range of 2.5–7.8. It should be noted that the ratio of p_1–p_2 to the kinetic pressure q

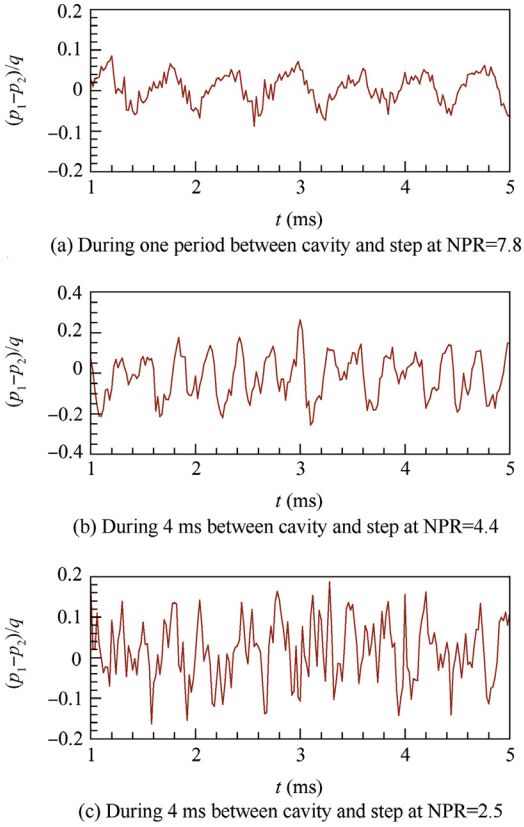

Fig. 12 Pressure differences fluctuations at different NPRs.

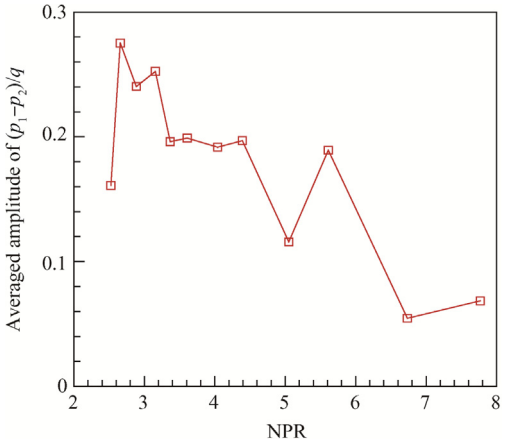

Fig. 13 Ratio of p_1–p_2 to q at different NPRs.

of flow in the exit section of nozzle is nearly 0.2 when the periodic jet oscillating appears.

The corresponding dominant frequency of fluctuating pressure in Fig. 11 is 3622 Hz, which can be read in the power spectrum density (PSD) of unsteady pressure shown in Fig. 14(a). Two harmonics also appear in this figure. A similar phenomenon is also observed from the PSD of the step (Fig. 14 (b)) where the dominant frequency is the same as that of the cavity.

The corresponding dominant frequency of the normalized fluctuating pressure difference between the cavity and the step in Fig. 12(a) is 1602 Hz, which can be read in the PSD of unsteady pressure shown in Fig. 15(a). The corresponding dominant frequency in Fig. 12(b) is 3501 Hz (Fig. 15(b)) and the corresponding dominant frequency in Fig. 12(c) is 2789 Hz (Fig. 15(c)). It should be argued that the dominant frequency of the normalized fluctuating pressure difference between the cavity and the step decreases with the NPR while the jet flipping appears.

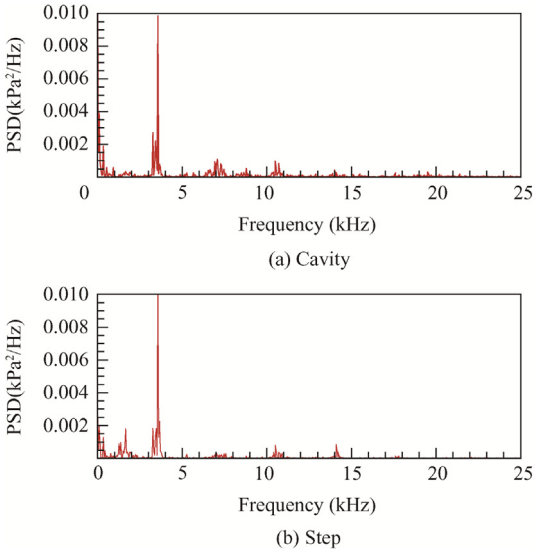

Fig. 14 Power spectrum density of unsteady pressure on the roofs of the cavity and the step at NPR = 4.4.

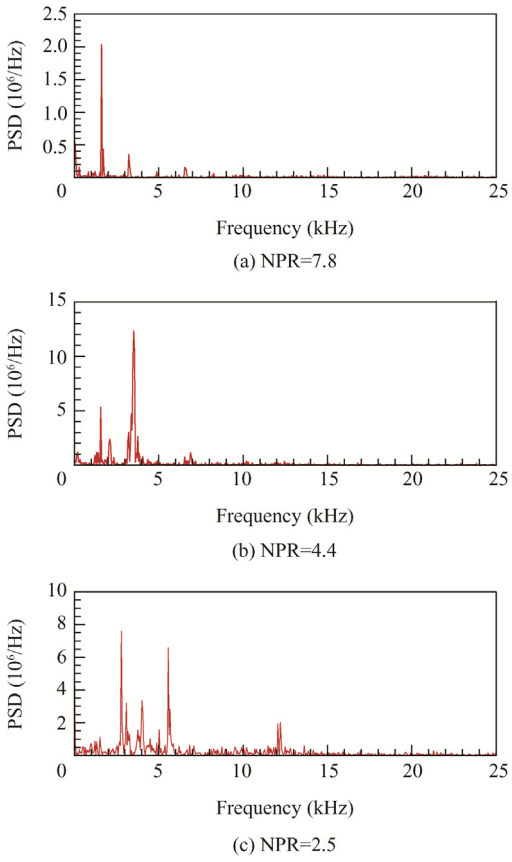

Fig. 15 Power spectrum density of the normalized unsteady pressure difference between the cavity and the step at different NPRs.

The dominant frequencies for some tested NPR cases are shown in Fig. 16. In addition to the dominant frequencies, two other sets of frequencies may be distinguished from the power spectrum. Firstly, there are peaks which are integral multiples of the dominant frequency (e.g. Fig. 14). These harmonics are not included in Fig. 16. Secondly, there are peaks in the spectra which occur at frequencies which are not simple multiples of the dominant frequency, and these are included in Fig. 16. The modified Rossiter modes expressed by

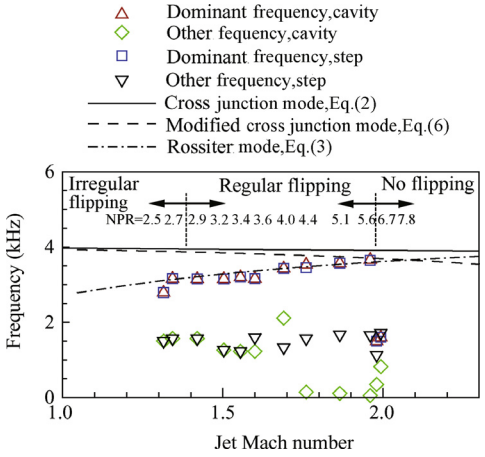

Fig. 16 Correlation of oscillating frequency vs nozzle exit Mach number.

Eq. (3), the cross junction mode expressed by Eq. (2), and the modified cross junction mode expressed by Eq. (6) are also shown. For the cross junction mode, the recovery temperature given by Eq. (5) was used as the air temperature in the cavity in Eq. (2). From this figure, it can be seen, from NPR = 2.9 to NPR = 5.6, the dominant frequency increases gradually from 3154 Hz to 3651 Hz, which is different from the trend given by the modified cross junction mode where the frequency decreases with the increase of the jet Mach number. It should be noted that the dominant frequencies of periodic jet flipping obtained from experimental data agree well with those from the modified Rossiter formula.

5. Conclusions

Wind tunnel tests were conducted from NPR = 2.5 to NPR = 7.8 in a vacuum-type wind tunnel for a novel supersonic fluidic oscillator which consisted of a 2D Laval nozzle with a divergence angle of 5°, a rectangular cavity, and a backward step. Schlieren videos, unsteady pressures on the roofs of the cavity and the step, and static pressures along the centerline of the oscillator were recorded for all the NPR cases. The experimental results show that:

(1) The supersonic jet periodic flipping between the cavity and the step appears from NPR = 2.9 to NPR = 5.6 according to schlieren visualization.
(2) The jet flipping appears only when the jet is over expanded.
(3) The dominant frequencies of jet flipping obtained from experimental data agree well with those from the modified Rossiter formula.

From the preliminary investigation, although the underlying mechanism for the cavity-actuated supersonic oscillator is not completely clear yet, some of its operation features can be summarized as follows: for a given cavity-step-actuated oscillator, it has an NPR scope for the flipping operation; the flipping frequency varies in a narrow range with the NPR (3154 Hz at NPR = 2.9 to 3651 Hz at NPR = 5.6), which is a potential advantage for flow control applications.

Further investigations and more detailed measurements are needed to find out the influencing factors of the flipping, and then to discover its mechanism and design an actuator based on this type of oscillator for flow control applications.

Acknowledgements

This study was supported by a grant from the Natural Science Foundation of Jiangsu Province (No. BK20150781). The authors wish to thank Prof. Tsutomu Saito and Dr. Kazuaki Hatanaka for their help.

References

1. Cattafesta LN, Sheplak M. Actuators for active flow control. *Annual Rev Fluid Mech* 2011;**43**:247–72.
2. Koklu. The effects of sweeping jet actuator parameters on flow separation control. Reston: AIAA; 2015. Report No.: AIAA-2015-2485.
3. Gregory WJ, Tomac MN. A review of fluidic oscillator development and application for flow control. Reston: AIAA; 2013. Report No.: AIAA-2013-2474.
4. Raghu S. Fluidic oscillators for flow control. *Exp Fluids* 2013;**54**:1455.
5. Ostermann. Phase-averaging methods for the natural flowfield of a fluidic oscillator. *AIAA J* 2015;**53**(8):2359–68.
6. Tomac MN, Greogory JW. Internal jet interactions in a fluidic oscillator at low flow rate. *Exp Fluids* 2014;**55**(5):646–56.
7. Carter V. Flueric temperature sensor. United States patent US 3667297. 1972 Jun 6.
8. Rockwell D, Naudascher E. Self-sustained oscillations of impinging free shear layers. *Annual Rev Fluid Mech* 1979;**11**:67–94.
9. Dequand S, Hulshoff SJ, Hirschberg A. Self-sustained oscillations in a closed side branch system. *J Sound Vibr* 2003;**265**(2):359–86.
10. Knowles RJ. Design analysis and test of fluidic communication components. 1971. Report No.: AD 767882.
11. Campagnuolo CJ, Lee HC. Review of some fluid oscillators. 1969. Report No.: AD0689445.
12. Raman G, Hailye M, Rice EJ. Flip-flop jet nozzle extended to supersonic flows. *AIAA J* 1993;**31**(6):1028–35.
13. Gokoglu SA, Kuczmarski MA, Culley DE, Raghu S. Numerical studies of a supersonic fluidic diverter actuator for flow control. Reston: AIAA; 2010. Report No.: AIAA-2010-4415.
14. Seele R, Graff E, Lin J, Wygnanski I. Performance enhancement of a vertical tail model with sweeping jet actuators. Reston: AIAA; 2013. Report No.: AIAA -2013-0411.
15. Sun B, Feng F, Wu XS, Luo XC. Experimental investigation of cavity-actuated supersonic oscillating jet. *Exp Therm Fluid Sci* 2015;**68**(5):155–62.
16. Sun B, Luo XC, Feng F, Wu XS. Experimental investigation on cavity-actuated under-expanded supersonic oscillating jet. *Chin J Aeronaut* 2015;**28**(5):1372–80.
17. Rockwell D, Naudascher E. Review of self-sustaining oscillations of flow past cavities. *J Fluids Eng* 1978;**100**(2):152–65.
18. Williams DR, Rowley CW. Recent progress in closed-loop control of cavity tones. Reston: AIAA; 2006. Report No.: AIAA-2006-0712.
19. Rossiter JE. Wind-tunnel experiments on the flow over rectangular cavities at subsonic and transonic speeds. London: Aeronautical Research Council; 1964. Report No.:3438.
20. Heller HH, Bliss DB. The physical mechanism of flow-induced pressure fluctuations in cavities and concepts for their suppression. Reston: AIAA; 1975. Report No.: AIAA-1975-0491.